Tectonophysics 691 (2016) 257–262

Contents lists available at ScienceDirect

Tectonophysics

journal homepage: www.elsevier.com/locate/tecto

Crustal deformation associated with the 2011 eruption of the Nabro volcano, Eritrea

Yariv Hamiel *, Gidon Baer

Geological Survey of Israel, Jerusalem, Israel

ARTICLE INFO

Article history:
Received 14 April 2016
Received in revised form 27 September 2016
Accepted 18 October 2016
Available online 28 October 2016

Keywords:
Nabro volcano
InSAR
Afar
Danakil
Deformation
Earthquakes
Faults
Dike

ABSTRACT

We investigate the crustal deformation associated with the 2011 eruption of the Nabro volcano, Afar, Eritrea. The Nabro volcano erupted on the night of 12 June 2011. A seismic sequence started 5 h before the onset of the volcanic eruption. It included 25 M > 3 earthquakes, of which one Mw 5.6 normal fault earthquake occurred on 12 June at about the same time as the onset of the eruption, and one Mw 5.6 strike-slip earthquake occurred at the end of the main sequence on 17 June. The deformation associated with the eruption and the seismic activity was resolved by Interferometric Synthetic Aperture Radar (InSAR) measurements of the TerraSAR-X and ENVISAT satellites. Interferograms were generated using ascending and descending track pairs. The Nabro caldera and the associated channel of magma flow are characterized by significant loss of coherence which limited our InSAR observations at the near field of the volcano. Therefore, detailed assessment of co- and post-eruptive seismicity and monitoring of post-eruptive deformation using continued InSAR observations were added to the co-eruptive analysis in order to better constrain the different magmatic and tectonic components and determine the final source model. We carried out tens of different inversion models. Our best-fit model includes a dike, a normal fault and a strike-slip fault, consistent with the mechanisms of the major earthquakes. Coulomb stress calculations based on our model are found to be in agreement with post-eruptive seismicity. Finally, the source mechanism and geometry of our model are found to be in accord with the major tectonic structures in this area.

1. Introduction

The Afar depression is located at the triple junction between the Red Sea, the Gulf of Aden and the East African rifts (Fig. 1), and accommodates the relative extensional deformation between the Arabian, Nubian, and Somalian plates (e.g., McKenzie et al., 1970). All three rifts tend to propagate obliquely to their main extensional directions (e.g. Boccaletti et al., 1998; Dauteuil et al., 2001; Corti, 2008; Agostini et al., 2009). Post-Oligocene volcanism in the Afar region is related to the activity of the Afar plume (e.g., Hoffman et al., 1997). The interaction between the three oblique rifts and the Afar lithospheric plume is the major cause for rift-axis as well as off-axis complex and distributed deformation and volcanic activity in the Afar region (e.g. Ebinger, 1989; Hayward and Ebinger, 1996; Manighetti et al., 1998; Bosworth et al., 2005).

The Danakil block is located within the Afar region (Fig. 1). It was suggested that this block was originally part of the Nubian plate until about 11 Ma ago, and since then was counter-clockwise rotated as a result of the interaction between the oblique rifts in this area (e.g. Chu and Gordon, 1998; Eagles et al., 2002). This interaction also implies oblique normal and strike-slip faulting along the Danakil block boundaries and probably across this block as well (Manighetti et al., 2001). Recent GPS measurements of interseismic deformation of the Afar region show that the Red Sea Rift diverges, with one segment along the main rift and the other along the western boundary of the Danakil block (McClusky et al., 2010). It was also suggested that the extensional rates of the major rift segments vary along strike. While north of 16°N latitude, extension (15 mm/yr) is focused on the main Red Sea Rift, south of 13°N, the extensional (20 mm/yr) axis has fully migrated to the western boundary of the Danakil block. These geodetic observations serve as an additional indication for oblique-slip and strike-slip deformation along the boundaries of the Danakil block.

The Nabro volcano is located within the Danakil block (Fig. 1). It is part of the Nabro Volcanic Range, a series of volcanoes crossing the Danakil block in the NNE-SSW direction, likely indicating the presence of internal deformation within this block (Wiart and Oppenheimer, 2005). An additional member of this volcanic range is the Mallahle volcano located several kilometers SSW of Nabro volcano (Fig. 1). In this paper we analyze the deformation associated with the 2011 eruption of Nabro volcano using Interferometric Synthetic Aperture Radar (InSAR) observations and modeling. A previous analysis of the co-eruptive deformation was presented by Goitom et al. (2015), and of the post-eruptive deformation by Hamlyn et al. (2014). In this paper we present

* Corresponding author.
E-mail address: yariv@gsi.gov.il (Y. Hamiel).

http://dx.doi.org/10.1016/j.tecto.2016.10.013
0040-1951/

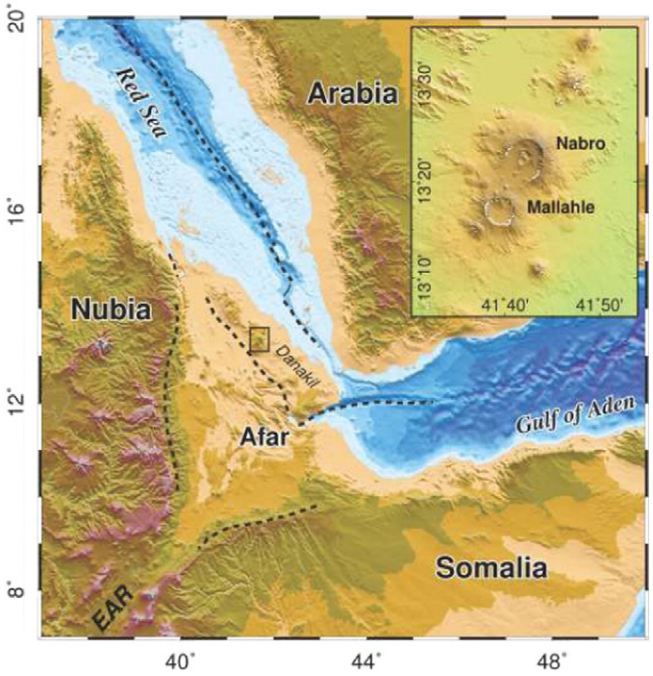

Fig. 1. Location map of the region showing the main tectonic features. Black dashed lines mark the location of the main rifts faults. Black box indicates the location of the insert map. Insert: Location map showing the Nabro volcano area.

a new, alternative source model that addresses both volcanic and seismic activity during the co-eruptive period, as well as the complex tectonics of the Danakil block. We first present measurements of the surface deformation during the main eruptive period and invert these observations to find a best-fit model. We then compare our best-fit model to co- and post-eruptive seismic activity near the Nabro volcano and to major tectonic features in this region. Finally, we discuss our new results in light of the model presented by Goitom et al. (2015).

2. The 2011 Nabro volcanic and seismic activity

The eruption of Nabro volcano started between 20:27 and 20:42 UTC on 12 June 2011. The volcano emitted ~4.5 Tg of sulfur dioxide (SO_2) (Theys et al., 2013), one of the highest levels ever recorded, and volcanic ash that reached a height of about 15 km and a distance of almost 2000 km away from the volcano. The major eruptive period lasted until 28 June, creating a ~13 km long lava flow channel that travelled northwestward through the open SW rim of the caldera (Goitom et al., 2015). Detailed report of the volcanic activity is presented by Goitom et al. (2015).

An M_L 4.8 earthquake occurred near Nabro volcano on 31 March 2011, about 2.5 months before the eruption (Goitom et al., 2015). No other $M > 2.1$ earthquake was identified in the days preceding the eruption. The Nabro seismic sequence began on 12 June, 15:37 UTC time, 5 h before the onset of volcanic eruption. It included 25 $M \geq 3$ earthquakes that occurred until 17 June (Fig. 2). Five of these earthquakes were larger than Mw 5, with two peak events of Mw 5.6. The first Mw 5.6 earthquake occurred on 12 June, 20:32 UTC time, probably during or just before the eruption onset. The second Mw5.6 earthquake occurred on 17 June, at the end of the main seismic sequence (Fig. 2). Three additional $Mw \geq 5$ normal faulting events occurred on 12 June (Fig. 2). Global Centroid Moment Tensor (CMT) solutions (Ekström et al., 2012) show NW-SE normal faulting and NNE-SSW (or WNW-ESE) strike-slip faulting (Fig. 2). The temporal evolution of seismic moment release was calculated using seismic data collected from global broadband networks (NEIC and EMSC catalogs). The total seismic moment that was accumulated during the earthquake sequence was 1×10^{18} Nm (Fig. 2).

Between 31 August and 7 October 2011 a local seismic network was operated near the Nabro volcano (Hamlyn et al., 2014). They relocated 456 earthquakes with local magnitudes in the range of $4.5 \geq M_L \geq -0.4$, including one M_L4.5 event, two events between $M_L = 3.0$ and 3.2, and others smaller than $M_L = 3$. Most of these earthquakes occurred below the Nabro and Mallahle volcanoes. The location of these events will be later related to our source model results (see Discussion below).

3. Results

3.1. InSAR observations

We analyzed the deformation associated with the 2011 Nabro event during its co-eruptive period and about 1 post-eruptive month. Post-eruptive data is mainly used to constrain the sources parameters and geometries. The co-eruptive deformation was captured by X-band images of TerraSAR-X satellite from DLR, Germany, whereas the post-eruptive deformation was captured by C-band ASAR images from the European Space Agency (ESA) ENVISAT satellite. The SAR data were processed using the JPL/Caltech ROI-PAC software (Rosen et al., 2004). Two interferometric pairs were processed to capture the entire co-eruptive deformation field (Fig. 3): a descending track interferogram from 11 June 2010 to 1 July 2011 (Fig. 3a), and an ascending track

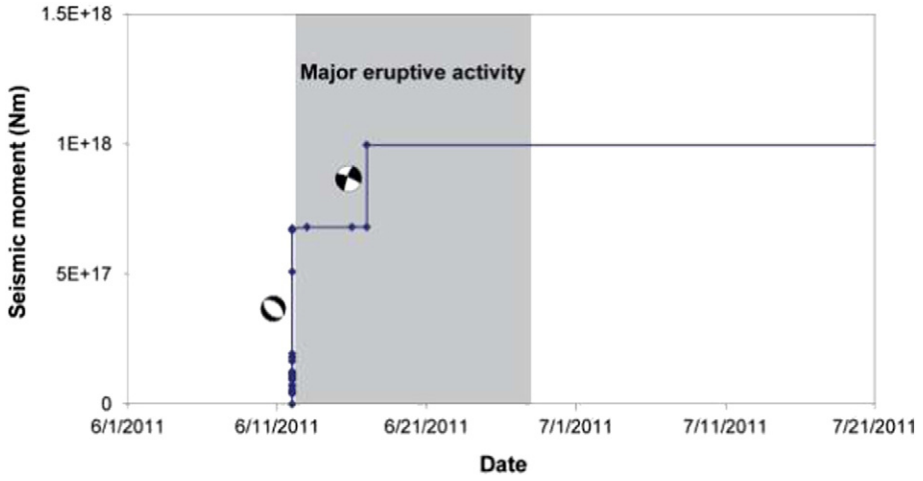

Fig. 2. Cumulative seismic moment released during the 2011 Nabro sequence. Main eruptive period is mark by gray area. Beach balls show the focal plane solutions for the two Mw5.6 peak events at the beginning (normal faulting) and the end (strike-slip faulting) of the main seismic sequence (Ekström et al., 2012).